Assessment of smart grid operation under emergency situations

Maria Fotopoulou [a], Dimitrios Rakopoulos [a,*], Stefanos Petridis [a] and Panagiotis Drosatos [a]

[a] *Chemical Process and Energy Resources Institute (CPERI), Centre for Research and Technology Hellas (CERTH), Greece*
** Corresponding author: Dimitrios Rakopoulos, email: rakopoulos@certh.gr , 52 Egialias Str., Maroussi, GR-15125 Athens, Greece.*

Abstract: Smart grids constitute a major trend of electrical networks, whose operation is underpinned by innovative optimization algorithms. Yet, sometimes, their normal operation is challenged by emergencies that require a Decision Support System (DSS) that modifies the Energy Management System (EMS) accordingly, taking into account the disconnected components. The purpose of this research is to assess the impact of emergencies on smart grids through a novel optimization algorithm. The algorithm comprises an optimizer, which maximizes the autonomy of the smart grid, prioritizing its Renewable Energy Sources (RES), and Artificial Neural Networks (ANN), which provide forecasts related to intermittent RES production. The assessment of each emergency includes the reduction of autonomy and sustainability of the smart grid's operation, with respect to curtailments, CO_2 emissions, etc. The algorithm is applied on a model of an actual smart grid in Spain, investigating a variety of cases in order to highlight the impact of each component's disconnection on the smart grid for various time intervals of the day. According to the results, an emergency affecting the smart grid's RES during noon might cause up to 46% reduction of its autonomy and an emergency affecting the storage might cause curtailments up to 25% of RES production.

Keywords: smart grid; emergency; assessment; autonomy; sustainability; optimization; artificial neural network; renewables; storage

1. Introduction

The ongoing energy transition has affected the concept of distribution networks, which have turned from passive, unidirectional and fuel-based architectures into active and sustainable smart grids [1,2]. This trend has established a research field related to the optimal management of the smart grid's resources [3,4], such as Renewable Energy Sources (RES), Battery Energy Storage Systems (BESS), local fuel-based generators, etc. Therefore, a variety of tools, algorithms and platforms have been developed in order to assist the operators of smart grids with the respective Energy Management System (EMS), forecasts, maintenance strategies, investments and decisions [5,6].

Yet, the main focus of the developed tools is the optimal daily operation, including energy market models, optimization of energy dispatch and power flow analysis [7,8]. Less attention is paid to the emergencies that might occur in a smart grid, the impact they might have on the system in terms of autonomy, sustainability and cost, and possible solutions to overcome these situations [9,10]. Nevertheless, this is an important topic, especially when the following factors are considered: i) the current energy crisis, ii) the lack of stability in systems with increased dependency on intermittent RES, and iii) the consumers' need for low System Average Interruption Duration Index (SAIDI) and System Average Interruption Frequency Index (SAIFI) [11].

There are many types of emergencies that a smart grid might face and many ways to handle them, depending on the nature and early detection of the issue [12]. For instance, a usual emergency is the partial blackout; a situation where part of the grid's generators, storage units, RES or load are disconnected and need repairs, while the energy dispatch is being modified [13]. Another example is the disconnection from the main grid, which requires islanded operation, if the smart grid's components support it. Also there might be a total blackout [14], where the smart grid's operator needs to perform black start. For this purpose, respective tools are developed, either individually or as part of a wider Decision Support System (DSS) for the operator.

In this context, Miao et al. [15] propose an emergency energy management especially designed for AC/DC microgrids in industrial parks, including a variety of Distributed Energy Resources (DER) and storage. The developed Mixed-Integer NonLinear Programming (MINLP) method has a multi-objective optimizer, the purpose of which is to: i) maximize the power supply to the load, ii) minimize the number of switching operations, and iii) minimize the cost of power generation. The authors display the performance of their algorithm in case the industrial park becomes islanded without a fault in the inner configuration and in case one of the generators is disconnected, while the park is islanded. In [16] an energy management strategy for microgrid emergency islanded operation is proposed. The strategy is rule-based and focuses on the cost of the modified operation during the emergency. Its performance is tested on a grid with DER, storage, residential load and Electric Vehicles (EVs), considering cases with adequate/inadequate reserve capacity and excessive RES generation. Also related to grids with EVs, in [17], an algorithm for handling outages due to natural disasters in small districts is presented. The study considers two commercial and residential buildings (four in total) with a shared parking station for their EVs. The purpose of the optimization algorithm is to minimize the cost, taking into account that the EVs can also be discharged. According to the results, the proposed energy management options can practically minimize the energy cost and improve energy resilience following blackouts. Furthermore, it is found that the EVs are capable of reducing energy cost by approximately 25% and supply the load during outages that last for seven hours. Following another approach, Lamedica et al. [18] present an innovative framework for the selection of electrical loads in smart buildings when the main power sources are limited or even totally absent due to an emergency situation. The control strategy is based on the Knapsack Problem. Results from Tabu Search, greedy heuristic and dynamic programming algorithms are compared to each other. According to the analysis, the authors state that the method of dynamic programming for an emergency scenario exhibits superior characteristics.

Furthermore, there are studies and algorithms where the emergencies need to be taken into account by a more general algorithm related to grid planning or optimal operation. For example, Lagrange et al. [19] aim to improve the electrical grid of a hospital to ensure the seamless operation of the surgery and the secure storage of safety stocks, by enabling its partial autonomy with a cost-efficient and sustainable way. The grid includes a Photovoltaic (PV) system, diesel generators and a BESS. The study examines two main objectives: i) the resilience of power supply when a power failure happens and ii) the optimization of the system in terms of the components' size to simultaneously attain economic profitability and resilience capacity. Based on the results, the hospital may save approximately $ 440,191 on average, over a 20-year life cycle of the facility, when PVs, BESS and diesel generators are installed. Emergencies may also be taken into account in day-ahead strategies, as in [20], where Das et al. propose a day-ahead optimal bidding strategy, taking into account uncertainties and outages of RES. The bidding model is optimized using MINLP and the uncertainties are modeled via probability density functions. The goal is to maximize the grid's profit with optimal risk management. The proposed strategy is tested on a grid with gas turbines, PVs, Wind Generators (WGs) and storages. In addition, the authors present an extensive risk analysis of expected bidding profits, including different associated "weights" and variations of RES production. Finally, Mansour - lakouraj et al. [21] propose a risk-based energy management for both normal and emergency operation, whose purpose is to minimize the operation cost. The test grid comprises generators, WGs and a storage system. It is highlighted that in order to generate scenarios for modeling the wind and real-time market price behaviors, the model uses the AutoRegressive Moving Average (ARMA). The authors examine a variety of emergencies, investigating the influence of the operator's risk.

It is evident that there is a variety of algorithms related to emergencies in smart grids. Yet, the vast majority of them focuses on cost minimization, neglecting the current energy crisis and the subsequent need for autonomy and sustainability, or focus in a specific case study, thus not providing a generalized solution. The purpose of this research is to present an algorithm for the optimal EMS of smart grids during an emergency, aiming to maximize its autonomy, prioritizing its RES production. Therefore, it expands the scope of [15–21], following the modern requirements for self-sufficiency. Furthermore, the developed algorithm not only proposes the optimal solution but

also assesses the impact of the emergency in terms of autonomy and sustainability, compared to normal operation. For this purpose, it utilizes an optimizer for the modified EMS and Artificial Neural Networks (ANN) for the forecast of unknown parameters (RES production), as in Figure 1. The algorithm is part of the DSS developed in the context of the European Horizon 2020 TIGON project [22] and is tested on one of its demo-grid's models, which is the smart grid of CIEMAT [23], located in Spain, including PVs, a WG, two BESS, a small diesel

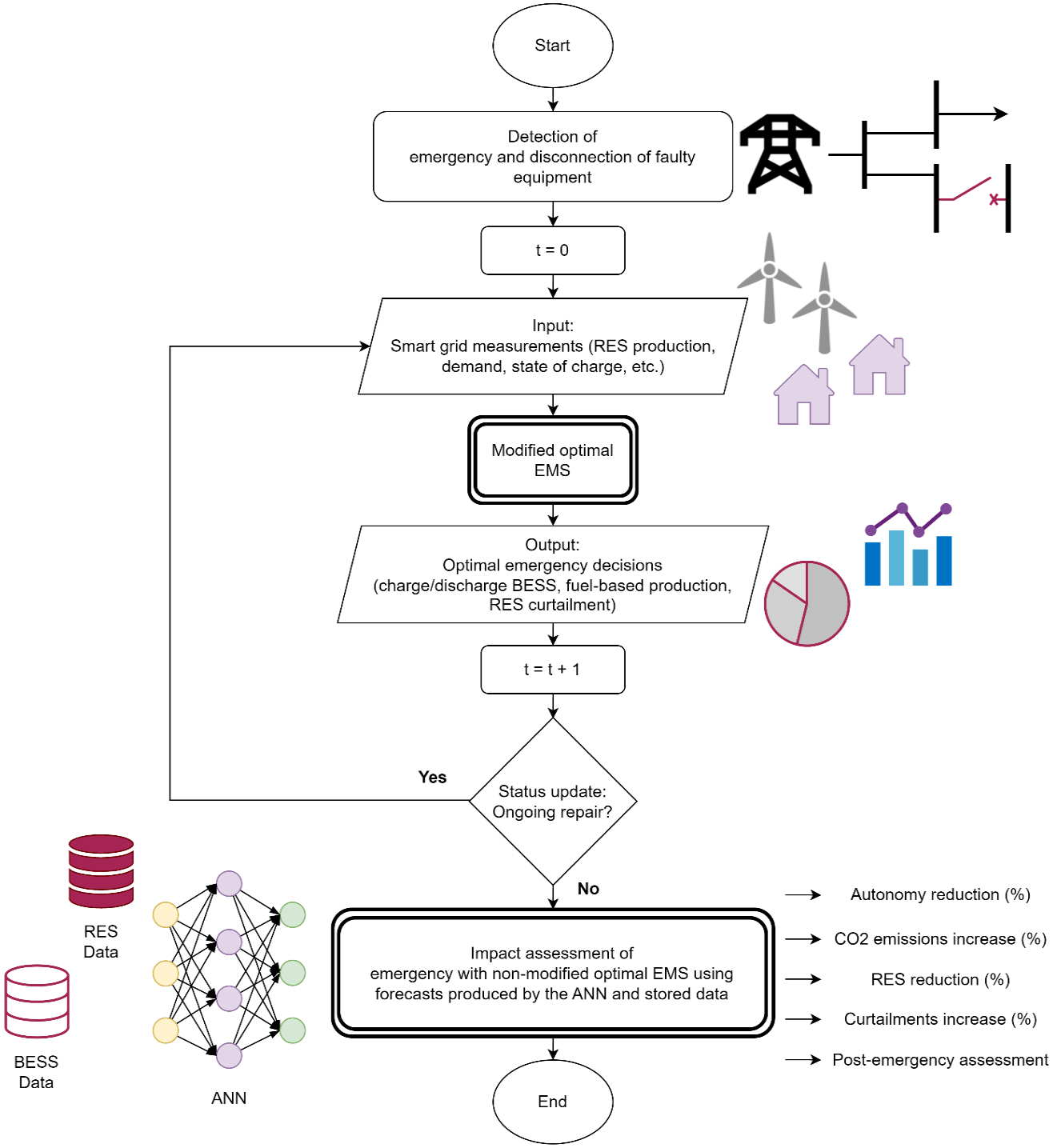

Figure 1: Flow chart of the proposed algorithm.

generator, residential load and EVs. The impact assessment of emergencies is performed for fifteen cases, each considering the disconnection of different major components. The evaluation criteria are the level of autonomy, the exhibited CO_2 emissions, RES contribution, curtailments and post-emergency assessment, which is mostly related to the status of the storage after the emergency.

2. Methodology

2.1 Algorithm description

The basic concept of the algorithm for handling emergencies and assessing their impact is presented in Figure 1. Once the emergency is detected, the faulty part of the smart grid, potentially including DER, BESS, etc., needs to be disconnected. Therefore, the optimizer is automatically modified, excluding the faulty component from the model, and uses the current smart grid measurements as input (PV and WG production, load, state of charge of the BESS, etc.). The output of the modified optimal EMS comprises the optimal decisions regarding: i) the charge/discharge of each BESS, ii) the fuel-based production and iii) RES curtailments, if required. The output refers to a certain time-step, which lasts for one hour, and needs to be directly applied to the smart grid. Once the time-step changes, the algorithm needs to be informed by the monitoring system about the status of the ongoing repairing actions. In case the repairing actions are not completed, the new smart grid measurements need to be used as input in order for the modified EMS to derive the optimal decisions for the new hourly time-step. The loop is repeated for as many time-steps as required until the repair is finished.

At that point, the impact of the emergency needs to be assessed. This is performed by comparing the results of the modified optimal EMS to the results that would have been provided by the normal EMS, if the emergency had been prevented. For this purpose, the normal EMS needs to use stored data, such as demand for the emergency's time-steps, or data that are not even available, such as the PV or the WG production that would have been measured in case these components had not been disconnected due to the emergency event. In order to generate the respective data, the algorithm incorporates two ANNs, one for the PV and one for the WG production. These ANNs are described in detail in sub-section 2.3. Finally, the results are compared in terms of autonomy, which is the objective of the smart grid's control, use of RES, CO_2 emissions, curtailments and post-emergency expected behavior.

2.2 Optimizer description

The basis of the algorithm is the optimizer, the objective (1) of which is to maximize the autonomy of the smart grid, using all available resources, prioritizing RES production for sustainability reasons. More specifically, the use of RES production has zero weight (as the optimal choice), thus not being included in the objective function. The second preferable supply units are the smart grid's BESS, since the optimizer considers them to be charged only by RES, presenting eco-friendly behavior. Therefore, the energy discharged from each BESS, D_b, has the lowest weight, w_1. The next preferable supply units are the smart grid's diesel generators, the production, G_g, of which has a higher weight than the BESS, w_2. For the sake of autonomy, the least preferable source is the main grid, the contribution, M, of which has the highest weight out of all sources, w_3. Finally, in order to ensure the maximum possible autonomy and the maximum use of RES production, the curtailed energy from each RES, R_r^{curt}, has the highest weight of all, w_4.

$$\min F = w_1 \sum_b D_b + w_2 \sum_g G_g + w_3 M + w_4 \sum_r R_r^{curt} \quad (1)$$

The objective function is limited by constraints that model the smart grid's components. Of course, when one or more components need to be disconnected, the respective decision variables and constraints are automatically removed from the EMS. In particular, constraints (2) - (6) refer to each BESS [24]. Constraint (2) is the energy

balance of each BESS, where S_b is the stored energy, S_b^{ini} is the initial stored energy at the current time-step, C_b is the energy charged to each BESS and η_b is the efficiency. Constraint (3) limits the stored energy of each BESS according to its minimum and maximum boundaries, S_b^{min} and S_b^{max}, respectively. The maximum energy that can be discharged from / charged to each BESS at each time-step is limited by the boundaries $D_b^{max}$and C_b^{max}, in constraints (4) and (5), where u_b^{dch} and u_b^{ch} are binary variables that indicate whether the BESS is discharged or charged, respectively. Finally, constraint (6) ensures that the BESS cannot be discharged and charged simultaneously.

$$S_b = S_b^{ini} + C_b\eta_b - D_b/\eta_b \tag{2}$$

$$S_b^{min} \leq S_b \leq S_b^{max} \tag{3}$$

$$D_b \leq D_b^{max} u_b^{dch} \tag{4}$$

$$C_b \leq C_b^{max} u_b^{ch} \tag{5}$$

$$u_b^{dch} + u_b^{ch} = 1 \tag{6}$$

Constraints (7) and (8) limit the contribution of each diesel generator, G_g, according to the maximum and minimum values, G_g^{max} and G_g^{min}, respectively, where u_g^{on} is the binary variable that indicates whether the diesel generator is activated or not.

$$G_g \leq G_g^{max} u_g^{on} \tag{7}$$

$$G_g \geq G_g^{min} u_g^{on} \tag{8}$$

Constraint (9) refers to the RES production of the r-th plant, R_r, which can either be used in the smart grid, R_r^{use}, or curtailed, R_r^{curt}.

$$R_r = R_r^{use} + R_r^{curt} \tag{9}$$

Finally, constraint (10) is the energy balance of the smart grid at each time-step, where L_l is the load of the l-th node.

$$\sum_l L_l + \sum_b C_b = \sum_b D_b + \sum_g G_g + \sum_r R_r^{use} + M \tag{10}$$

Regarding the load, it should be highlighted that it might comprise both usual building-related consumption, e.g., heating and lights, and Electric Vehicle (EV) demand [25]. The energy balance of an EV, v, while moving, at each time-step, is presented in (11), where S_v is the stored energy in its battery, S_v^{ini} is the initial stored energy, D_v is the energy required for transportation and η_v is the EV's efficiency. When being charged, the energy balance is presented in (12), where C_v is the energy drawn from the grid to charge the EV. Certainly, as in all storage systems, the stored energy is limited by the minimum and maximum technical boundaries, S_v^{min} and S_v^{max}, respectively, presented in (13), while the maximum energy that can be charged to each EV per time-step is limited by (14). Finally, the survey of the European Commission found in [26] suggests that the time intervals when EV owners are willing to charge their vehicles follow the profile, P_t, presented in (15). This profile can be helpful especially when the operator needs to derive profiles for EV charging and aggregate them to the overall load of the smart grid.

$$S_v = S_v^{ini} - D_v/\eta_v \tag{11}$$

$$S_v = S_v^{ini} + C_v\eta_v \tag{12}$$

$$S_v^{min} \le S_v \le S_v^{max} \tag{13}$$

$$C_v \le C_v^{max} \tag{14}$$

$$P_t = \begin{cases} 100\%, t \in [00{:}00, \quad 06{:}00) \cup [22{:}00, \quad 00{:}00) \\ 10\%, \quad t \in [06{:}00, \quad 08{:}30) \cup [18{:}00, \quad 22{:}00) \\ 50\%, t \in [08{:}30, \quad 18{:}00) \end{cases} \tag{15}$$

Overall, this constitutes a Mixed Integer Linear Programming (MILP) problem. The results of the proposed methodology have been verified with the use of PowerFactory, DIgSILENT [27], on models of the demo-grids of the TIGON project.

2.3 ANN description

For the forecast of unknown parameters, which in this case are the PV and WG production, the algorithm uses the output of two ANNs respectively [28,29]. ANNs are a type of machine learning algorithm modeled after the structure and function of the human brain [30] and consist of interconnected processing nodes, known as artificial neurons, which are organized in layers.

An artificial neuron is the fundamental unit of an ANN. It functions as a simple processing node that receives input signals, performs computations, and produces an output signal [31]. Each artificial neuron receives input signals from other neurons through its incoming synapses, each represented by a weight value to denote the respective strength. The neuron computes the weighted sum of its inputs and applies an activation function to determine whether to produce an output signal. The output signal is then passed to its adjacent neurons through its outgoing synapses. The combination of these simple processing nodes organized in a network structure allows ANNs to perform complex computations and make predictions based on patterns of the input data.

The output of a single artificial neuron is calculated as follows:

$$y = f((\sum_j w_j x_j) + b) \tag{16}$$

, where x_j and w_j are the input signal and the weight of the incoming synapses, respectively, for the neuron's j-th edge. Moreover, b is the neuron's bias, f the neuron's activation function and y the neuron's output. The weights and bias represent the trainable parameters of the neuron and can change their values to achieve a certain behavior on the output when provided with a certain input.

The structure of an ANN, when multiple neurons are combined in layers, is depicted in Figure 2. Three types of layers can be found in an ANN: i) the input layer, where a vector of values is provided to the ANN as input, ii) the hidden layers, which contain the majority of ANN's neurons to perform computations, and iii) the output layer, where the output vector is produced, after the input processing by the hidden layers. ANNs are trained using supervised learning, according to which the network is provided with a labeled dataset and the algorithms optimize the weights of the neurons' edges to minimize the error between the predicted output and the actual output [32]. This process is repeated for multiple iterations to refine the model's accuracy.

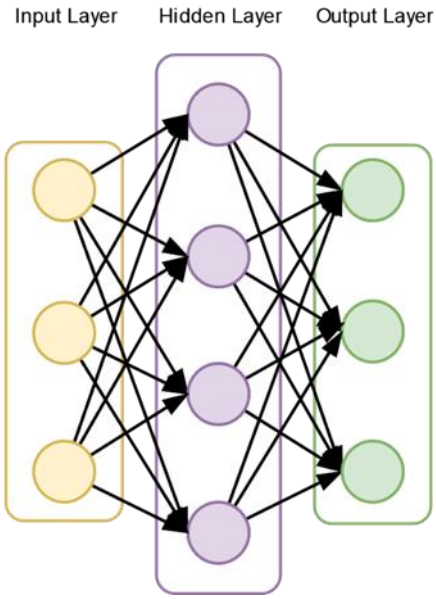

Figure 2: Graphical structure depicting an ANN with one input layer, one hidden layer and one output layer.

Table 1: Parameters of the developed ANNs.

	Inputs	Hidden layer neurons	Outputs
PV model	3	10	1
WG model	1	5	1

For the purposes of this study, two different ANNs are trained for forecasting PV and WG production. Their characteristics are presented in Table 1. The inputs of the PV model, to yield the PV production, are the direct and diffuse irradiance, and the ambient temperature for the PV's location. The input of the WG model, to yield the wind production, is the wind speed for the WG's location. The activation function used in the hidden and output layers for both models is the Rectified Linear Unit (ReLU) [33].

The ANN models were created using the Tensorflow 2.0 library [34], in Python programming language [35]. For processing the data, pandas and scikit-learn libraries were utilized [36,37].

3. Smart grid analysis

3.1 Smart grid components

The current state of CIEMAT's smart grid consists of a PV system, a WG, a main and a secondary BESS and a load, which presents a peak power equal to 20.7 kW, as in Table 2 [38,39]. Furthermore, for the purposes of this study, CIEMAT's smart grid is considered to also include EVs, following the recent trends in electric traction, and a small diesel generator [40,41] to enhance the system's autonomy by covering the basic/lowest demand. In particular, taking into account the average travelling distance [42], the percentage of EVs in Spain [43,44], the load peak [45], the charging time preferences [26] and the specifications of EV batteries [46], it can be concluded that a realistic approach is the consideration of two EVs, which charge evenly in the time interval [22:00-00:00) with an overall demand of 4 kWh.

Table 2: CIEMAT's smart grid basic components.

Component	Nominal values
RES	
PV	Installed system: 22.14 kW, average daily production: 106 kWh [38]
WG	Installed system: 3.5 kW, average daily production: 27 kWh [38]
BESS	
BESS 1	Pb-acid BESS, Maximum stored energy: 60 kWh, technical minimum: 16.7%
BESS 2	LiFePo BESS, Maximum stored energy: 24 kWh, technical minimum: 37.5%
Fuel-based generators	
Diesel generator	Nominal power: 5 kW [40], Minimum (for efficient operation): 30% [41]
Load	
Basic load	20.7 kW peak, following the daily curve of [39]
EVs	Two EVs [46], maximum stored energy: 40 kWh, consumption: 166 Wh/km

3.2 ANN training and accuracy on the examined smart grid

Given the location of the examined grid, data input from [38] are used for both ANNs, forming two datasets for identical components as the ones used in this study. The first one includes the hourly direct and diffuse irradiance, temperature and PV production throughout a reference year, while the second one includes the wind speed and WG production. Each dataset contains 8,760 data points. In both cases, 80% of the data points are selected randomly for training purposes, whereas the remaining 20% are used for testing the trained models.

Before training, a form of normalization named min-max feature scaling [47] is applied to scale the training data points into the range [0,1], as shown in (17).

$$x_i^{train,norm} = \frac{x_i^{train} - x^{train,min}}{x^{train,max} - x^{train,min}} \tag{17}$$

, where x_i^{train} and $x_i^{train,norm}$ represent the value of the i-th row of the training set, before and after normalization, respectively, and $x^{train,max}$ and $x^{train,min}$ represent the maximum and minimum values in the training set. Normalizing the data before training is a frequent procedure, since it improves the neural network's performance and convergence speed. Scaling all the inputs to have values in comparable ranges prevents any particular feature from having a disproportionate effect on the overall learning process [48].

For testing the model, a similar normalization procedure takes place for the testing data as shown in (18):

$$x_i^{test,norm} = \frac{x_i^{test} - x^{train,min}}{x^{train,max} - x^{train,min}} \tag{18}$$

, where x_i^{test} and $x_i^{test,norm}$ represent the value of the i-th row of the testing set, before and after normalization, respectively.

The ANNs are trained with the built-in version of Adam [49], which is an optimization algorithm that extends Stochastic Gradient Descent [50]. The purpose of the training process is to minimize the Root-Mean-Square Error (RMSE) between the forecasted and the real values. The RMSE formula is provided in (19):

$$RMSE = \sqrt{\frac{\sum_i (F_i - A_i)^2}{n}} \tag{19}$$

, where F_i and A_i are the forecasted and the actual values, respectively, for training set's i-th element and n is the number of data points in the training set.

For evaluating the performance of the trained models, Mean Absolute Percentage Error (MAPE) is used, which is a metric commonly used for the evaluation of forecasting models. The PV model achieves a MAPE of 3.9% in the testing set, which is equal to the performance of other models found in literature [28]. The WG, on the other hand, has a MAPE performance of 14%, which is acceptable according to literature, where the usual performance is between 10% and 20% [29]. It needs to be mentioned that results of forecasting models are highly depended on the dataset's quality. Indicative results of the models' predictions are presented in Figure 3 - Figure 4.

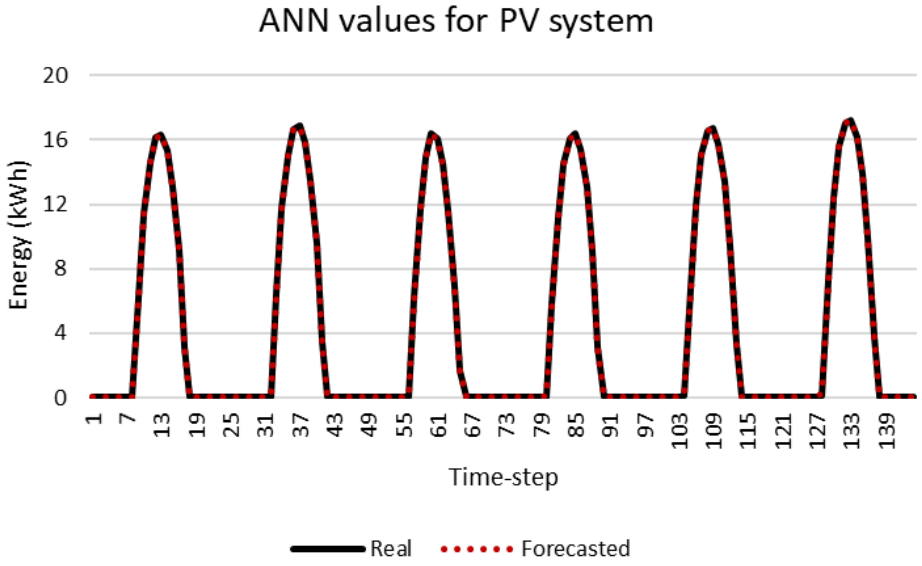

Figure 3: PV predictions using ANN.

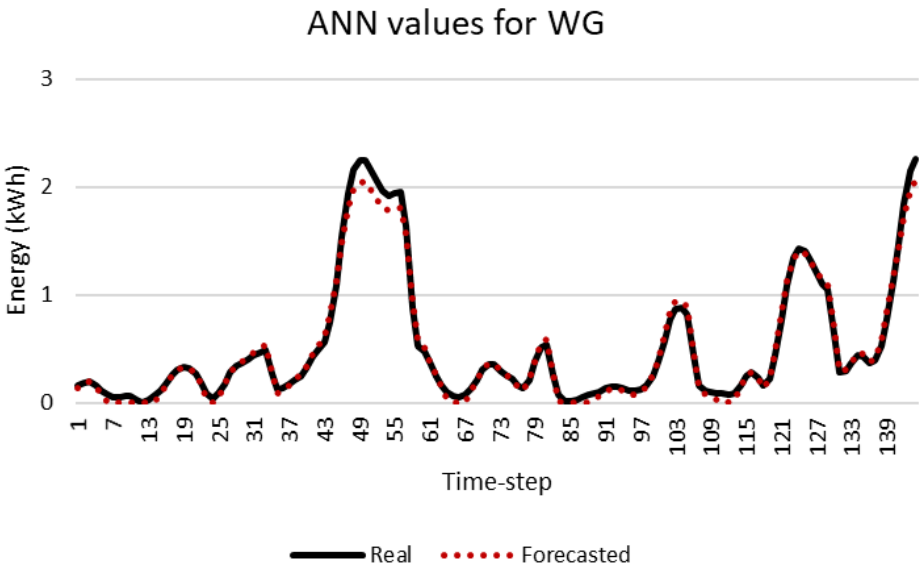

Figure 4: WG predictions using ANN.

3.3 Simulated representative day and emergency cases' definition

The expected operation of a representative day in the examined smart grid is presented in Figure 5. The representative day is selected upon the daily RES production. In particular, the PV production on that day is equal to 112 kWh and the WG production is equal to 26 kWh, close to the average daily values over a year, i.e., 106 kWh and 27 kWh, respectively. The RES contribute to the energy mix mostly during noon, while the BESS, which are solely charged from the RES, are fully discharged before the end of the day. Therefore, they are assumed to be at their technical minimum State of Charge (SOC) in the beginning of the day. The diesel generator covers the demand when the RES production and BESS contribution is not enough. If all of the aforementioned sources are not enough to cover the load, then energy is supplied by the main grid.

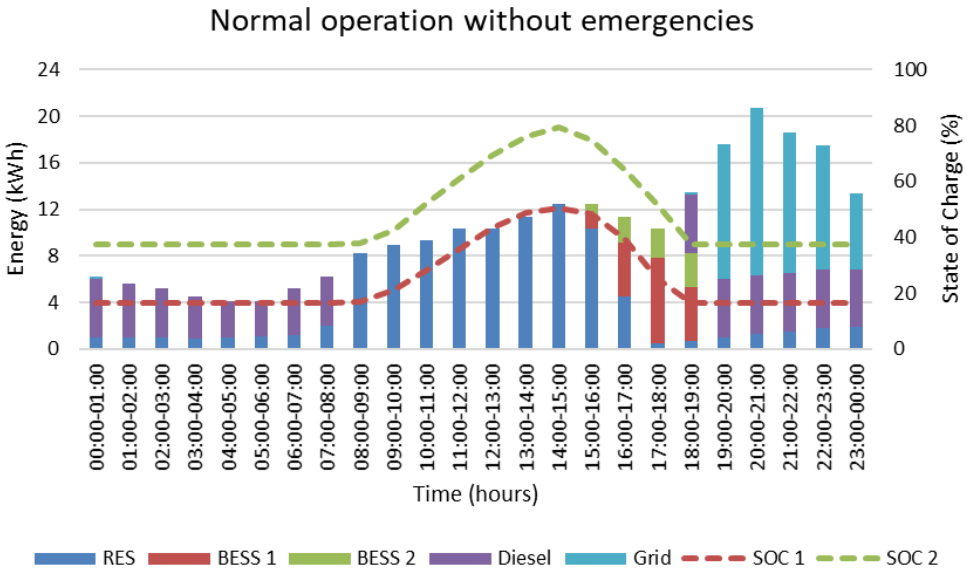

Figure 5: Expected daily operation of the smart grid, in case of no emergencies.

Table 3: Definition of emergency cases.

	Disconnected component	Duration
Emergencies affecting the smart grid's RES		
Case 1	PV + WG	All day
Case 2	PV	All day
Case 3	WG	All day
Case 4	PV + WG	11:00 - 16:00
Case 5	PV	11:00 - 16:00
Case 6	WG	11:00 - 16:00
Emergencies affecting the smart grid's BESS		
Case 7	BESS 1 + BESS 2	All day
Case 8	BESS 1	All day
Case 9	BESS 2	All day
Case 10	BESS 1 + BESS 2	15:00 - 19:00
Case 11	BESS 1	15:00 - 19:00
Case 12	BESS 2	15:00 - 19:00
Emergencies affecting the smart grid's diesel generator		
Case 13	Diesel generator	All day
Case 14	Diesel generator	00:00 - 08:00
Case 15	Diesel generator	18:00 - 00:00

Table 3 describes the emergency cases considered in this study. These emergencies are assumed to happen both all day and during the hours each component contributes mostly to the energy mix. Furthermore, in the framework of the sustainability assessment, the specific CO_2 emissions of the diesel generator and grid are considered to be equal to 800 gr/kWh [51,52] and 166 gr/kWh [53], respectively, since the main grid of Spain has high RES penetration.

4. Results

4.1 Autonomy and sustainability assessment

The assessment of the system's autonomy and sustainability for all cases considered is presented in Table 4. The results provide quantitative evaluation for three parameters during each emergency along with comparison against the respective values, when normal operation is considered: i) the autonomy during each emergency, ii) the use of the smart grid's RES both directly and indirectly through the BESS and iii) the CO_2 emissions required for the modified operation. Detailed results for each case's baseline are presented in Table 5. Furthermore, Table 6 presents the curtailment of RES production, which may be required if the BESS are disconnected when they would normally be in charging mode. Table 7 presents the post-emergency assessment in the cases where the stored energy after the emergency is different than it would be if the emergency was prevented.

Overall, it can be concluded that the loss of both RES during noon hours (when their contribution to the load is maximized), i.e., case 4, decreases the smart grid's autonomy during the emergency by 46%, while their all-day loss, i.e., case 1, decreases the autonomy by 38%. Separate results are also given for the loss of each RES, individually, where it is shown that the loss of the PV system has a higher impact than the loss of the WG. This is expected because the PV system produces daily more energy, even though the WG produces all day. However, the most important finding is that the loss of RES during noon hours, either entirely or partially, affects the post-emergency capabilities of the smart grid, as presented in Table 7. More specifically, such emergencies, i.e., case 4 – case 6, cause the discharge of both BESS, which would otherwise be charged with the surplus RES production. Therefore, the useable stored energy at the end of the emergency ranges from 0 kWh to 23 kWh instead of 28 kWh.

Table 4: Autonomy and sustainability assessment.

	Autonomy (kWh)	Autonomy (%)	Autonomy reduction (%)	RES use (kWh)	RES use reduction (%)	CO_2 emissions (kg)	CO_2 emissions increase (%)
Emergencies affecting the MG's RES							
Case 1	118 kWh	48%	38%	0 kWh	100%	116 kg	97%
Case 2	139 kWh	56%	28%	26 kWh	80%	108 kg	84%
Case 3	175 kWh	70%	10%	106 kWh	18%	68 kg	15%
Case 4	31 kWh	54%	46%	9 kWh	84%	22 kg	N/A
Case 5	34 kWh	60%	40%	14 kWh	75%	20 kg	N/A
Case 6	57 kWh	100%	0%	57 kWh	0%	0 kg	N/A
Emergencies affecting the MG's BESS							
Case 7	178 kWh	72%	8%	104 kWh	20%	71 kg	20%
Case 8	185 kWh	75%	4%	117 kWh	10%	65 kg	11%
Case 9	192 kWh	78%	0%	130 kWh	0%	59 kg	0%
Case 10	33 kWh	70%	30%	16 kWh	62%	16 kg	298%
Case 11	37 kWh	77%	23%	25 kWh	40%	11 kg	180%
Case 12	40 kWh	85%	15%	34 kWh	19%	6 kg	60%
Emergencies affecting the MG's diesel generator							
Case 13	130 kWh	52%	33%	130 kWh	0%	20 kg	-67%
Case 14	9 kWh	22%	78%	9 kWh	0%	5 kg	-79%
Case 15	16 kWh	16%	64%	16 kWh	0%	14 kg	-57%

Table 5: Autonomy and sustainability baseline.

	Related cases	Autonomy (kWh)	Autonomy (%)	RES use (kWh)	CO_2 emissions (kg)
All day	1 - 3, 7 - 9, 13	192 kWh	78%	130 kWh	59 kg
[00:00 - 08:00)	14	41 kWh	99%	9 kWh	26 kg
[11:00 - 16:00)	4 - 6	57 kWh	100%	57 kWh	0 kg
[15:00 - 19:00)	10 - 12	47 kWh	100%	42 kWh	4 kg
[18:00 - 00:00)	15	46 kWh	45%	16 kWh	33 kg

Table 6: Curtailments assessment.

	Curtailments (kWh)	Increase of curtailments (%)
Emergencies affecting the smart grid's BESS, whole day emergencies		
Case 7	35 kWh (25% of production)	N/A (0 kWh normally)
Case 8	17 kWh (13% of production)	N/A (0 kWh normally)
Case 9	0 kWh (0% of production)	N/A (0 kWh normally)

Table 7: Post-emergency assessment.

	Usable stored energy after the emergency (kWh)	Usable stored energy without emergency (kWh)
Emergencies affecting the smart grid's RES during peak production and noon demand [11:00 - 16:00)		
Case 4	0 kWh	28 kWh
Case 5	0 kWh	28 kWh
Case 6	23 kWh	28 kWh
Emergencies affecting the smart grid's BESS during discharge [15:00 - 19:00)		
Case 10	30 kWh	0 kWh
Case 11	20 kWh	0 kWh
Case 12	10 kWh	0 kWh

The loss of the system's BESS might decrease the autonomy of the smart grid up to 30%, which is observed in case 10, when the two BESS are disconnected during all of the hours that they should be discharged. The same case also presents the highest reduction of RES energy usage, i.e., 62%, and the highest CO_2 emissions increase, i.e., 298%, out of all emergencies related to BESS. Furthermore, according to Table 6, the whole day loss of the system's BESS can lead to curtailments reaching up to 25% of RES production, i.e., 35 kWh.

Finally, out of all cases, the diesel generator affects the autonomy of the smart grid the most, i.e., by 78%, for emergencies happening in the beginning of the day (case 14) when the RES produce little energy and the BESS are empty. Therefore, the loss of the diesel generator means that the energy that would be produced by it needs to be injected from the main grid, hence the vast decrease of autonomy. Also, the emergencies related to the diesel generator, i.e., cases 13-15, are the only ones that reduce the CO_2 emissions, This is attributed to the fact that the main grid of Spain has an energy mix rich in RES, with lower emissions per kWh than the diesel generator.

4.2 Detailed analysis of extreme cases

After presenting the values related to the impact assessment of all defined cases, this sub-section aims to showcase the detailed results of the algorithm during some of the most extreme emergencies. Figure 6 presents the detailed results related to case 4, where both RES are disconnected during noon hours, having a great impact on the smart grid's autonomy, CO_2 emissions and post-emergency capability. The selected time-interval (noon) includes both RES overall peak production and load peak during noon. The absence of RES is replaced mostly by the BESS in the beginning of the emergency and then by the diesel generator and the main grid. As a result, the demand,

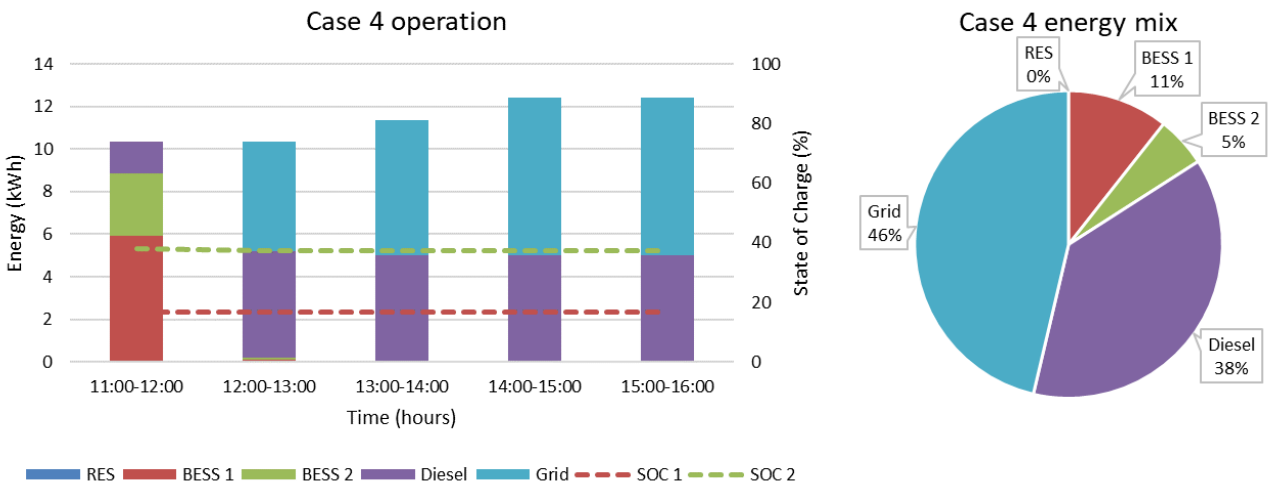

Figure 6: Smart grid operation and energy mix for Case 4 (PV + WG disconnection 11:00 - 16:00).

which would otherwise be mostly covered by PV production, is covered by the main grid, 46%, the diesel generator, 38%, and the two BESS, only 11% and 5%, respectively. Also, the SOC of both BESS reaches their technical minimum, instead of increasing.

Case 8, where BESS 1 is disconnected throughout the day is also interesting to analyze further, as it does not only require curtailments, but also challenges the limits of the other BESS, as presented in Figure 7 and Figure 8. More specifically, when the RES production exceeds the demand, BESS 2 is being charged with all the energy that should normally be provided to both BESS. However, since BESS 2 has limited capacity, it soon reaches its maximum SOC and all the remaining available energy, 17 kWh (13% of RES production), is curtailed. As a result, the demand is covered 42% by the RES, 28% by the diesel generator, 25% by the main grid and only 5% by BESS 2.

Furthermore, regarding BESS-related emergencies, it is critical to further analyze the modified operation of the smart grid in case 10, where both BESS are disconnected when they should be discharged, i.e., 15:00 – 19:00. As previously described, this is an extreme case because it compromises the autonomy during the emergency by 30% and increases the CO_2 emissions by 298%. The detailed results of case 10 are presented in Figure 9. It is noted that

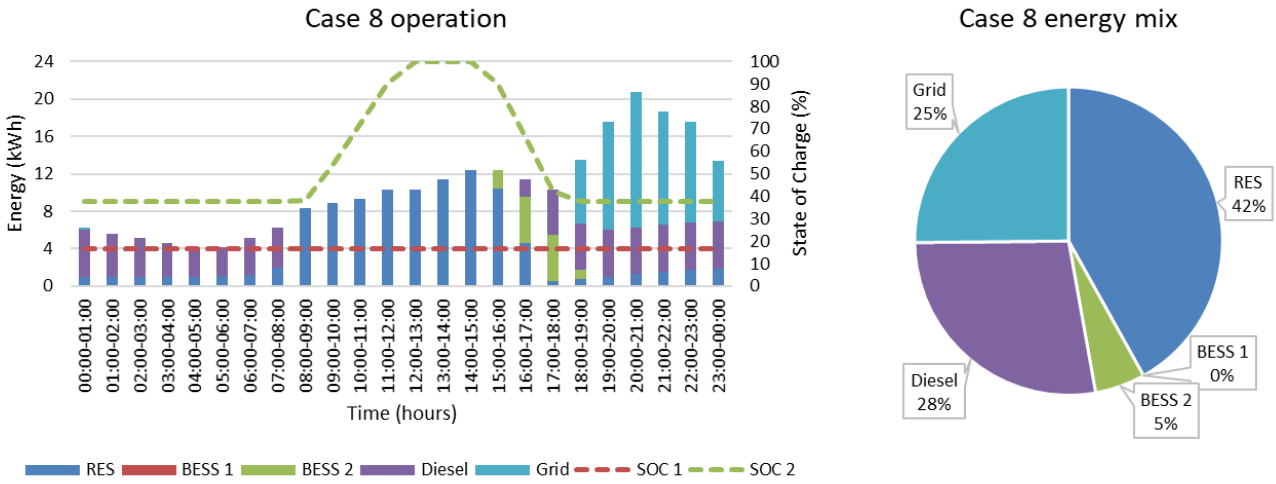

Figure 7: Smart grid operation and energy mix for Case 8 (BESS 1 disconnection, all day).

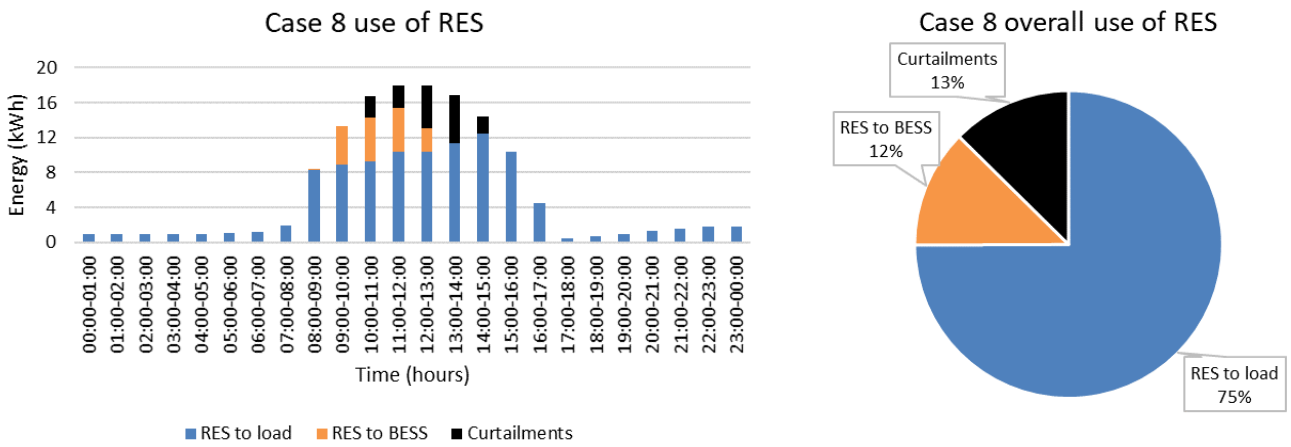

Figure 8: Use of RES for Case 8 (BESS 1 disconnection, all day).

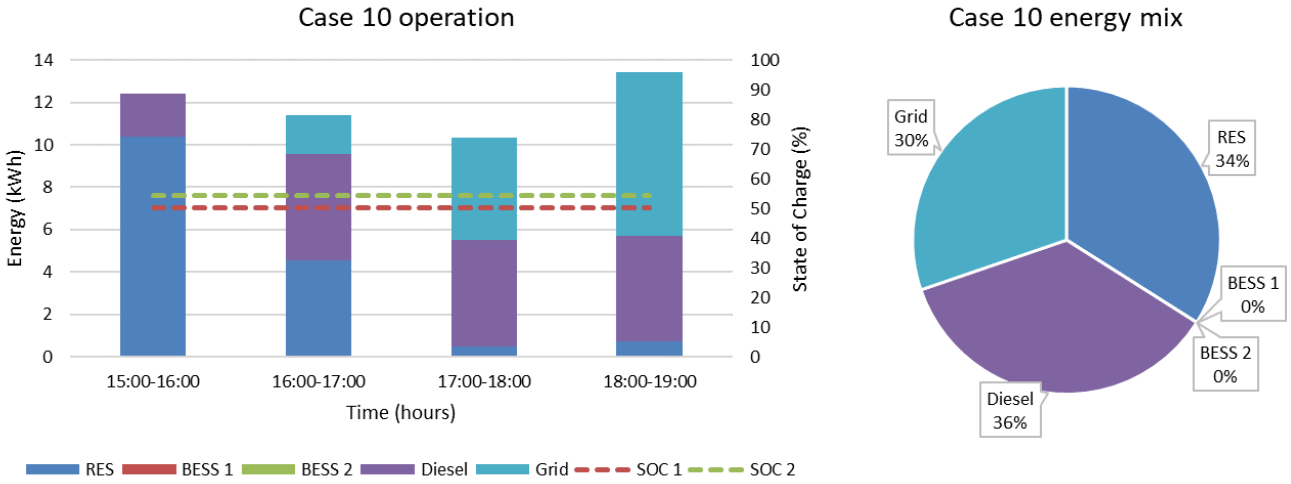

Figure 9: Smart grid operation and energy mix for Case 10 (BESS 1 and BESS 2 disconnection 15:00 - 19:00).

the BESS are replaced by the diesel generator, in order to preserve the smart grid's autonomy as much as possible, and when its maximum production is not sufficient either, the demand is covered by the main grid. As a result, the demand is covered 36% by the diesel generator, 34% by RES and 30% by the main grid. Yet, it is highlighted that once the two BESS are reconnected they shall have 30 kWh usable stored energy, instead of 0 kWh, which is also mentioned in Table 7. Therefore, the negative impact of their disconnection can be compensated by their reconnection at 19:00.

Finally, case 15, which focuses on the loss of the diesel generator during the peak of the load, including the hours when the EVs are fully charged, is presented in Figure 10. In this case, the production of the WG is low and the contribution of the BESS is insufficient to cover the demand. Therefore, 84% of the demand is covered by the main grid. This reduces the autonomy by 64%. The rest of the demand is covered by the WG, 8%, and by the two BESS, 5% and 3% respectively.

5. Conclusions

This paper presents a novel algorithm for handling emergencies in smart grids and assessing their impact. It comprises an optimizer that maximizes the autonomy of the smart grid, supported by an ANN-based forecaster. The

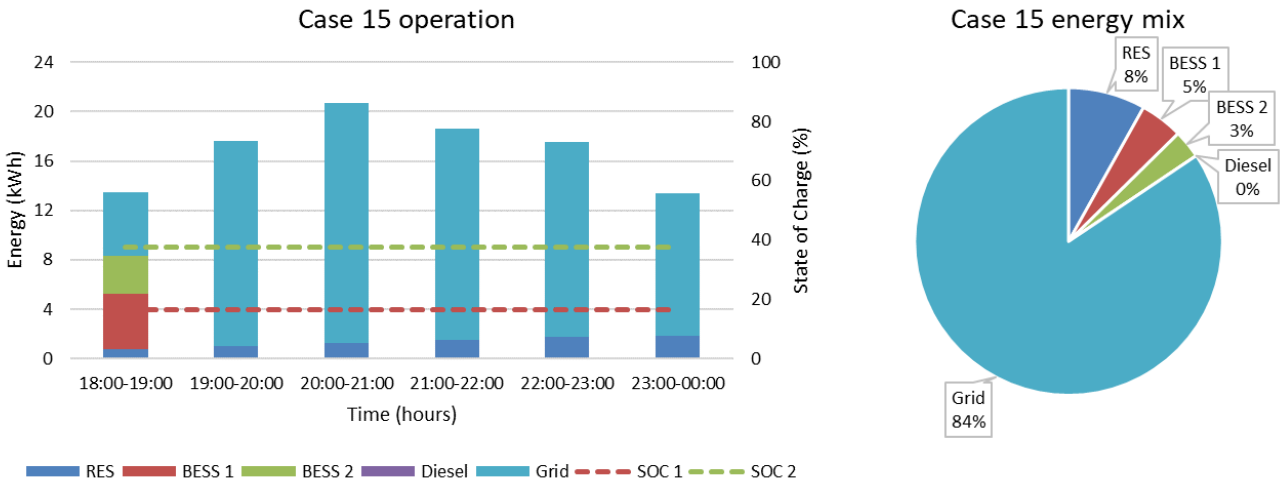

Figure 10: Smart grid operation and energy mix for Case 15 (diesel disconnection 18:00 - 00:00).

algorithm is part of the DSS developed in the context of the European Horizon 2020 TIGON project and is tested on a model of the project's demo-grid, located in Spain. The results showcase the impact of various emergencies related to the disconnection of major components, such as PVs, BESS, etc., on the smart grid's autonomy and sustainability. It is found that an emergency affecting the smart grid's RES during noon might cause up to 46% reduction in its autonomy, while an emergency affecting the BESS might cause curtailments up to 25% of RES production. In addition, the study showcases the importance of having a rich mix of energy sources and storage systems, which may cover, either fully or partially, the demand in case one component needs to be disconnected. Regarding the CO_2 emissions, it is noted that even though the diesel generator is beneficial for the smart grid's autonomy, it may be more harmful for the environment in comparison to the energy injected from the main grid if the latter incorporates enough RES production to have lower emissions per kWh.

The algorithm is verified with the use of PowerFactory and is expected to be applied on the actual demo-grid of the project in the next months. The actual monitored results are expected to be incorporated in a future publication, validating the proposed solution in real-life conditions. Additionally, combinations of emergencies, e.g., PVs and BESS, are considered to be studied in future work.

Declaration of competing interest

The authors declare that they have no known competing financial interests or personal relationships that could have appeared to influence the work reported in this paper.

Data availability

Data will be made available on request.

Acknowledgements

This research has received funding from the European Union's Horizon 2020 research and innovation programme, TIGON (Towards Intelligent DC-based hybrid Grids Optimizing the Network performance), under grant agreement No 957769, https://cordis.europa.eu/project/id/957769. This research was supported by CIEMAT, and especially Mr. Oscar Izquierdo and Ms. Paula Peña Carro, who provided us with the main parameters of their MG. In addition, this research was supported by CARTIF, and especially Dr. Luis Ángel Bujedo and Mr. Juan Jesús Samaniego Muñoz, as the researchers of CARTIF provided us with the PowerFactory model of the MG in the context of the TIGON project.

Nomenclature

Acronyms

ANN	Artificial Neural Network
ARMA	AutoRegressive Moving Average
BESS	Battery Energy Storage System
DER	Distributed Energy Resources
DSS	Decision Support System
EMS	Energy Management System
EV	Electric Vehicle
MAPE	Mean Absolute Percentage Error
MILP	Mixed Integer Linear Programming
MINLP	Mixed Integer NonLinear Programming
PV	Photovoltaic
ReLU	Rectified Linear Unit
RES	Renewable Energy Sources
RMSE	Root Mean Squared Error
SAIDI	System Average Interruption Duration Index
SAIFI	System Average Interruption Frequency Index
WG	Wind Generator

Symbols

A	Actual/real value
C	Energy charged to storage
D	Energy discharged from storage
F	Forecasted value
G	Production of generator
L	Load
M	Main grid
P	Profile
R	Energy from RES
S	Stored energy
b	Neuron's bias
f	Activation function
n	Number of data points in the training set
u	Binary decision variable
w	Weight
x	Value of the dataset
y	Neuron's output

Greek Letters

η	Efficiency

Superscipts and Subscripts

b	Index of BESS
ch	Charge of storage
$curt$	Curtailment
dch	Discharge of storage
g	Index of generators
i	Rows of dataset
ini	Initial value
j	Neuron's edge

l	Index of nodes
max	Maximum value
min	Minimum value
$norm$	Normalized value
on	Activation of generator
r	Index of RES
t	Time
$test$	Value of testing Set
$train$	Value of training Set
use	Used energy
v	Index of EVs

References

[1] Lund H, Østergaard PA, Connolly D, Mathiesen BV. Smart energy and smart energy systems. Energy 2017;137:556–65. https://doi.org/10.1016/j.energy.2017.05.123.

[2] Jalali MM, Kazemi A. Demand side management in a smart grid with multiple electricity suppliers. Energy 2015;81:766–76. https://doi.org/10.1016/j.energy.2015.01.027.

[3] Olabi AG. Renewable energy and energy storage systems. Energy 2017;136:1–6. https://doi.org/10.1016/j.energy.2017.07.054.

[4] Olabi AG, Onumaegbu C, Wilberforce T, Ramadan M, Abdelkareem MA, Al – Alami AH. Critical review of energy storage systems. Energy 2021;214:118987. https://doi.org/10.1016/j.energy.2020.118987.

[5] Tsao Y-C, Thanh V-V, Lu J-C. Multiobjective robust fuzzy stochastic approach for sustainable smart grid design. Energy 2019;176:929–39. https://doi.org/10.1016/j.energy.2019.04.047.

[6] Lund H, Andersen AN, Østergaard PA, Mathiesen BV, Connolly D. From electricity smart grids to smart energy systems – A market operation based approach and understanding. Energy 2012;42:96–102. https://doi.org/10.1016/j.energy.2012.04.003.

[7] Alirezazadeh A, Rashidinejad M, Abdollahi A, Afzali P, Bakhshai A. A new flexible model for generation scheduling in a smart grid. Energy 2020;191:116438. https://doi.org/10.1016/j.energy.2019.116438.

[8] Kaygusuz A. Closed loop elastic demand control by dynamic energy pricing in smart grids. Energy 2019;176:596–603. https://doi.org/10.1016/j.energy.2019.04.036.

[9] Woon KS, Phuang ZX, Taler J, Varbanov PS, Chong CT, Klemeš JJ, et al. Recent advances in urban green energy development towards carbon emissions neutrality. Energy 2023;267:126502. https://doi.org/10.1016/j.energy.2022.126502.

[10] Murphy PM, Twaha S, Murphy IS. Analysis of the cost of reliable electricity: A new method for analyzing grid connected solar, diesel and hybrid distributed electricity systems considering an unreliable electric grid, with examples in Uganda. Energy 2014;66:523–34. https://doi.org/10.1016/j.energy.2014.01.020.

[11] Personal E, Guerrero JI, Garcia A, Peña M, Leon C. Key performance indicators: A useful tool to assess Smart Grid goals. Energy 2014;76:976–88. https://doi.org/10.1016/j.energy.2014.09.015.

[12] Fotopoulou M, Rakopoulos D, Petridis S. Decision Support System for Emergencies in Microgrids. Sensors 2022;22:9457. https://doi.org/10.3390/s22239457.

[13] Moya O. Energy management systems (EMS): use in emergency conditions. Proceedings of the 1990 IEEE Colloquium in South America, Argentina, Brazil, Chile, Uruguay: IEEE; 1990, p. 168–72. https://doi.org/10.1109/COLLOQ.1990.152824.

[14] Barakat S, Emam A, Samy MM. Investigating grid-connected green power systems' energy storage solutions in the event of frequent blackouts. Energy Reports 2022;8:5177–91. https://doi.org/10.1016/j.egyr.2022.03.201.

[15] Miao M, Li Y, Wang Z, Ouyang L, Liu F, Lee KY, et al. An Emergency Energy Management for AC/DC Micro-grids in Industrial Park. IFAC-PapersOnLine 2018;51:251–5. https://doi.org/10.1016/j.ifacol.2018.11.710.

[16] Azim R, Hantao Cui, Fangxing Li. Power management strategy combining energy storage and demand response for microgrid emergency autonomous operation. 2016 IEEE PES Asia-Pacific Power and Energy Engineering Conference (APPEEC), Xi'an, China: IEEE; 2016, p. 2620–5. https://doi.org/10.1109/APPEEC.2016.7779964.
[17] Tian M-W, Talebizadehsardari P. Energy cost and efficiency analysis of building resilience against power outage by shared parking station for electric vehicles and demand response program. Energy 2021;215:119058. https://doi.org/10.1016/j.energy.2020.119058.
[18] Lamedica R, Santini E, Teodori S, Romito DZ. Electrical loads management in energy emergency conditions. International Journal of Electrical Power & Energy Systems 2015;66:86–96. https://doi.org/10.1016/j.ijepes.2014.10.038.
[19] Lagrange A, de Simón-Martín M, González-Martínez A, Bracco S, Rosales-Asensio E. Sustainable microgrids with energy storage as a means to increase power resilience in critical facilities: An application to a hospital. International Journal of Electrical Power & Energy Systems 2020;119:105865. https://doi.org/10.1016/j.ijepes.2020.105865.
[20] Das S, Basu M. Day-ahead optimal bidding strategy of microgrid with demand response program considering uncertainties and outages of renewable energy resources. Energy 2020;190:116441. https://doi.org/10.1016/j.energy.2019.116441.
[21] Mansour-lakouraj M, Shahabi M. Comprehensive analysis of risk-based energy management for dependent micro-grid under normal and emergency operations. Energy 2019;171:928–43. https://doi.org/10.1016/j.energy.2019.01.055.
[22] TIGON n.d. https://tigon-project.eu/ (accessed February 25, 2023).
[23] CIEMAT. Centro de Investigaciones Energéticas, Medioambientales y Tecnológicas n.d. https://www.ciemat.es/ (accessed February 25, 2023).
[24] Mohiti M, Monsef H, Lesani H. A decentralized robust model for coordinated operation of smart distribution network and electric vehicle aggregators. International Journal of Electrical Power & Energy Systems 2019;104:853–67. https://doi.org/10.1016/j.ijepes.2018.07.054.
[25] Fotopoulou M, Rakopoulos D, Blanas O. Day Ahead Optimal Dispatch Schedule in a Smart Grid Containing Distributed Energy Resources and Electric Vehicles. Sensors 2021;21:7295. https://doi.org/10.3390/s21217295.
[26] European Commission. Joint Research Centre. Institute for Energy and Transport., TRT Trasporti e Territorio Srl. Projections for electric vehicle load profiles in Europe based on travel survey data. LU: Publications Office; 2013.
[27] PowerFactory - DIgSILENT n.d. https://www.digsilent.de/en/powerfactory.html (accessed February 12, 2023).
[28] Theocharides S, Makrides G, Livera A, Theristis M, Kaimakis P, Georghiou GE. Day-ahead photovoltaic power production forecasting methodology based on machine learning and statistical post-processing. Applied Energy 2020;268:115023. https://doi.org/10.1016/j.apenergy.2020.115023.
[29] Nazir MS, Alturise F, Alshmrany S, Nazir HafizMJ, Bilal M, Abdalla AN, et al. Wind Generation Forecasting Methods and Proliferation of Artificial Neural Network: A Review of Five Years Research Trend. Sustainability 2020;12:3778. https://doi.org/10.3390/su12093778.
[30] McCulloch WS, Pitts W. A logical calculus of the ideas immanent in nervous activity. The Bulletin of Mathematical Biophysics 1943;5:115–33. https://doi.org/10.1007/BF02478259.
[31] Rosenblatt F. The perceptron: A probabilistic model for information storage and organization in the brain. Psychological Review 1958;65:386–408. https://doi.org/10.1037/h0042519.
[32] Russell SJ (Stuart J 1962-. Artificial intelligence : a modern approach. Third edition. Upper Saddle River, N.J. : Prentice Hall, [2010] ©2010; 2010.
[33] Agarap AF. Deep Learning using Rectified Linear Units (ReLU) 2019.
[34] Martín Abadi, Ashish Agarwal, Paul Barham, Eugene Brevdo, Zhifeng Chen, Craig Citro, et al. TensorFlow: Large-Scale Machine Learning on Heterogeneous Systems 2015.
[35] Python programming language. Python n.d. https://www.python.org/.
[36] team T pandas development. pandas-dev/pandas: Pandas. Zenodo; 2020. https://doi.org/10.5281/zenodo.3509134.

[37] Pedregosa F, Varoquaux G, Gramfort A, Michel V, Thirion B, Grisel O, et al. Scikit-learn: Machine Learning in Python. Journal of Machine Learning Research 2011;12:2825–30.
[38] Renewables Ninja n.d. https://www.renewables.ninja/ (accessed February 14, 2023).
[39] Conseil international des grands réseaux électriques, editor. Benchmark systems for network integration of renewable and distributed energy resources. Paris: CIGRÉ; 2014.
[40] 5kW (6kVA) Silent Diesel Generator, 1 Phase/3 Phase. ATO n.d. https://www.ato.com/5kw-silent-diesel-generator#:~:text=5kW%20(6kVA)%20diesel%20generator%20for,AC%20voltage%20can%20be%20chosen (accessed February 14, 2023).
[41] Diesel Generator. ScienceDirect n.d. https://www.sciencedirect.com/topics/engineering/diesel-generator (accessed February 14, 2023).
[42] Eurostat. Passenger Mobility Statistics n.d. https://ec.europa.eu/eurostat/statistics-explained/index.php?title=Passenger_mobility_statistics#Distance_covered (accessed February 14, 2023).
[43] Spain: Plug-In Car Sales Maintain 10% Share. INSIDEEVs n.d. https://insideevs.com/news/584466/spain-plugin-car-sales-april-2022/ (accessed February 14, 2023).
[44] Number of vehicles per household in the United States from 2001 to 2017. Statista n.d. https://www.statista.com/statistics/551403/number-of-vehicles-per-household-in-the-united-states/ (accessed February 12, 2023).
[45] de Almeida A, Fonseca P. Residential Monitoring to Decrease Energy Use and Carbon Emissions in Europe 2006.
[46] Nissan Leaf. Electric Vehicle Database n.d. https://ev-database.org/car/1106/Nissan-Leaf (accessed February 14, 2023).
[47] Patro SGK, sahu KK. Normalization: A Preprocessing Stage. International Advanced Research Journal in Science, Engineering and Technology 2015:20–2. https://doi.org/10.17148/IARJSET.2015.2305.
[48] Sola J, Sevilla J. Importance of input data normalization for the application of neural networks to complex industrial problems. IEEE Trans Nucl Sci 1997;44:1464–8. https://doi.org/10.1109/23.589532.
[49] Kingma DP, Ba J. Adam: A Method for Stochastic Optimization 2017.
[50] Ruder S. An overview of gradient descent optimization algorithms. ArXiv Preprint ArXiv:160904747 2016.
[51] The Carbon-Footprint of Diesel Generators. FEA n.d. https://www.feace.com/single-post/the-carbon-footprint-of-diesel-generators (accessed February 14, 2023).
[52] JCM Proposed Methodology - Displacement of Grid and Captive Genset Electricity by a Small-scale Solar PV System n.d.
[53] Carbon intensity of the power sector in Spain from 2000 to 2021. Statista n.d. https://www.statista.com/statistics/1290486/carbon-intensity-power-sector-spain/ (accessed February 14, 2023).